

# ROBUSTNESS OF RATE-BASED CONGESTION CONTROL ALGORITHM FOR ABR SERVICE CLASS IN ATM NETWORKS

Hiroyuki Ohsaki, Masayuki Murata and Hideo Miyahara

Department of Information and Computer Sciences  
Faculty of Engineering Science, Osaka University  
1-3 Machikaneyama, Toyonaka, Osaka 560, Japan  
oosaki@ics.es.osaka-u.ac.jp

**Abstract** — A rate-based congestion control algorithm has been developed and standardized in the ATM forum for ABR service class. In the standard, the behavior of source and destination end systems is specified by several control parameters such as *RIF* (Rate Increase Factor) and *RDF* (Rate Decrease Factor). In spite of the fact that the performance of the rate-based congestion control algorithm heavily depends on the selection of these control parameters, the selection method of parameters is not shown in the standard. In this paper, by extending our previous work, appropriate settings of rate-control parameters in the various circumstances are investigated. We first analyze the dynamical behavior of the rate-based congestion control for multiple groups of ABR connections with different propagation delays. We then evaluate the effect of CBR traffic on ABR connections.

## I. INTRODUCTION

A rate-based congestion control algorithm has been standardized for ABR (Available Bit Rate) service class by the ATM forum [1, 2, 3]. In the standard document [1], several control parameters are defined for controlling cell transmission at the source end system. These include *RIF* (Rate Increase Factor) and *RDF* (Rate Decrease Factor) that control rate increase and decrease envelopes. During a connection establishment process, the source end system negotiates these control parameters with the network. In [4], we have shown that effectiveness of the rate-based congestion control is heavily dependent on a choice of control parameters. If control parameters are configured properly, the rate-based congestion control can achieve high performance (i.e., no buffer overflow, high link utilization and small cell delay). However, a selection method of control parameters has not been specified in the standard, and parameters should be determined intuitively unless a proper tool is provided.

In [5], we have shown the analytic method to determine an appropriate setting of control parameters including *RIF*, *RDF* and *ICR* (Initial Cell Rate) for a single-hop network configuration. In the analysis, we have assumed that all source end systems behave identically, and that they always have cells to transmit. Under these assumptions, we have derived conditions that control parameters should satisfy to achieve two main objectives: preventing cell loss and achieving full link utilization. Based on these results, we have proposed a simple guideline

for parameter tuning at the ATM Forum [6]. In addition to obtain high performance (in terms of cell loss and link utilization), fairness among connections is also an important issue. Actually, each connection may have a different round-trip delay according to the network configuration. In such a case, fairness among connections may be degraded due to the different feedback delays. When another ABR connection is newly established in the network, the ramp-up time of this connection is also important.

We further need to consider existence of real-time applications such as audio and video in a multimedia network environment. Since these applications use CBR (Constant Bit Rate) or VBR (Variable Bit Rate) service class, multiple service classes co-exist in the network. For ABR service class to utilize the available bandwidth unused by CBR/VBR service class, CBR/VBR traffic should be given higher priority than ABR traffic at the switch to guarantee QoS (Quality of Service) requirements of CBR/VBR traffic. Namely, cells of ABR traffic are awaited in the switch buffer if a CBR/VBR cell exists in the switch buffer in the case that the switch has two logically independent buffers — one for CBR/VBR service class and the other for ABR service class. In other words, the bandwidth available to the ABR service class is limited by CBR/VBR traffic. Therefore, when a CBR/VBR connection is newly added into the network, the bandwidth available to the ABR service class is suddenly decreased, which would give a serious effect on the performance of the ABR connections; the switch buffer for ABR cells may become overloaded for a while leading to a large queue buildup and eventually cell losses due to the buffer overflow.

In this paper, we focus on the two subjects. We first analyze the behavior of the rate-based congestion control for a single-hop network but each group of connections is allowed to have the different propagation delay. In [7], Blot et al. have analyzed a dynamical behavior of a rate-based congestion control for connections with different propagation delays. However, their analytic model was quite simple and different from the rate-based congestion control standard [1]. Through numerical examples, we show the effect of control parameters on the ramp-up time of a new ABR connection. We next derive the maximum queue length at the switch after a new CBR connection is established in the network.

The rest of this paper is organized as follows. In Section II, we first analyze the behavior of the rate-based congestion control for a single-hop network with a simple *binary-mode switch* [2] but each group of connections is allowed to have a different propagation delay. In Section III, we then analyze the maximum queue length at the switch after a new CBR connection is established in the network. In Section IV, we present some concluding remarks.

## II. MULTIPLE GROUPS OF CONNECTIONS

In this section, we derive the dynamical behavior of the rate-based congestion control for  $N$  groups of connections with different propagation delays. Through numerical examples, we show the importance of parameter tuning for achieving good fairness and the short ramp-up time for an additional ABR connection.

### A. Analysis

We divide ABR connections into  $N$  groups with different propagation delays. Within a group, connections have identical propagation delays. Figure 1 depicts our analytic model in the case of  $N = 2$ . Propagation delays from each source to the switch, and from the switch to each destination of group  $n$  ( $1 \leq n \leq N$ ) are denoted by  $\tau_{sx n}$  and  $\tau_{xd n}$ , respectively. For brevity, we introduce  $\tau_n (= 2\tau_{sx n} + 2\tau_{xd n})$  and  $\tau_{xds n} (= \tau_{sx n} + 2\tau_{xd n})$ . The number of connections in group  $n$  is denoted by  $N_{VC n}$ . We assume that all connections in each group behave identically. Namely, all connections in each group have the same control parameters. Let us introduce  $RIF_n$ ,  $RDF_n$  and  $N_{RM n}$  as  $RIF$ ,  $RDF$  and  $N_{RM}$  of group  $n$ , respectively. We also assume  $\tau_{sx i} \leq \tau_{sx j}$  and  $\tau_{xd i} \leq \tau_{xd j}$  for any  $i$  and  $j$  ( $i < j$ ) without loss of generality.

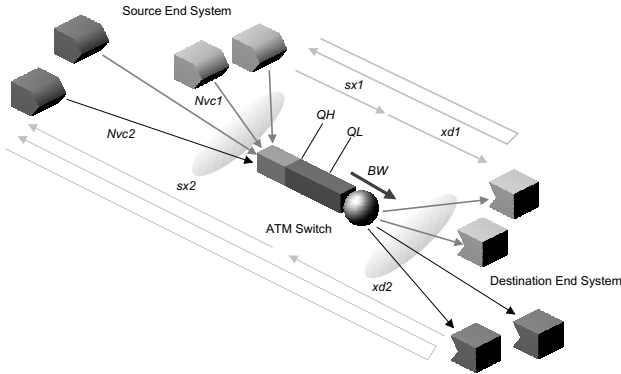


Fig. 1: Analytic Model for Multiple Groups for  $N = 2$ .

Let us introduce  $ACR^n(t)$  and  $Q(t)$  that represent  $ACR$  of the source end system in group  $n$  and the queue length at the switch observed at time  $t$ , respectively. As shown in Fig. 2,  $ACR^n(t)$  and  $Q(t)$  have periodicity. We further introduce  $ACR_i^n(t)$  and  $Q_i(t)$  as the  $ACR^n(t)$  and  $Q(t)$  in Phase  $i$ , which are defined as

$$ACR_i^n(t) = ACR^n(t - t_{i-1}),$$

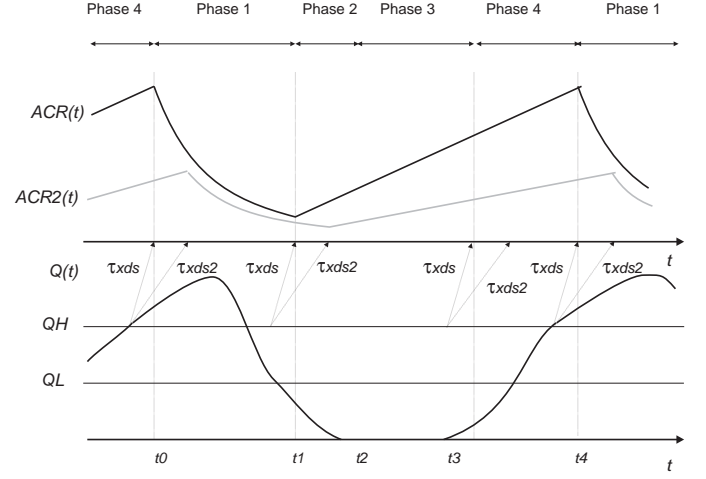


Fig. 2: Pictorial View of  $ACR^n(t)$  and  $Q(t)$ .

$$Q_i(t) = Q(t - t_{i-1}).$$

Because of the difference in propagation delays between the switch and the source via the destination ( $\tau_{xds n}$ ), congestion information from the switch arrives at the sources at different time. Hence, by defining  $\Delta$  as  $\tau_{xds n} - \tau_{xds 1}$ ,  $ACR_i^n(t)$  is obtained as follows (see [5] for the details of derivations).

$$\begin{aligned} ACR_1^n(t) &= ACR_1^n(\Delta) e^{-\frac{BW RDF_n}{N_{VC} N_{RM n}}(t-\Delta)} \\ ACR_2^n(t) &= ACR_2^n(\Delta) + \frac{BW RIF_n PCR}{N_{VC} N_{RM n}}(t - \Delta) \\ ACR_3^n(t) &\cong ACR_3^n(\Delta) e^{\frac{RIF_n PCR}{N_{RM n}}(t-\Delta)} \\ ACR_4^n(t) &= ACR_4^n(\Delta) + \frac{BW RIF_n PCR}{N_{VC} N_{RM n}}(t - \Delta) \end{aligned}$$

for

$$\Delta \leq t \leq \Delta + t_{i-1,i}.$$

At time  $t$ , the switch observes  $ACR^n(t - \tau_{sx n})$  for group  $n$  because of the propagation delay from the source to the switch,  $\tau_{sx n}$ . Therefore,  $Q_i(t)$  in Phase  $i$  is obtained as

$$\begin{aligned} Q_i(t) &= \max(Q_i(\tau_{sx 1}) \\ &+ \int_{\tau_{sx 1}}^t \left( \sum_{n=1}^N N_{VC n} ACR_i^n(x - \tau_{sx n}) - BW \right), 0), \\ &\tau_{sx 1} \leq t < \tau_{sx 1} + t_{i-1,i}. \end{aligned}$$

The duration of Phase  $i$ ,  $t_{i-1,i}$ , is obtained as follows.

$$t_{i-1,i} = \begin{cases} Q_1^{-1}(Q_L) + \tau_{xds 1} & i = 1 \\ \min(Q_2^{-1}(Q_H) + \tau_{xds 1}, Q_2^{-1}(0) + \tau_{xds 1}) & i = 2, 4 \\ ACR_3^{n-1}(BW/N_{VC}) + \tau & i = 3 \end{cases}$$

where  $ACR_i^{n-1}(t)$  and  $Q_i^{-1}(t)$  are defined as the inverse representations of  $ACR_i^n(t)$  and  $Q_i(t)$ , respectively.

### B. Numerical Examples

In this subsection, we provide several numerical examples. To exhibit the effect of the rate-control parameters on the ramp-up

time of an additional ABR connection, we first add connections of group 1 in the network. After these connections are stabilized, another connection of group 2 with  $ICR = PCR/20$  is established. The number of connections for each group is set to  $N_{VC1} = 10$  for group 1 and  $N_{VC2} = 1$  for group 2. We fixed the bandwidth of bottleneck link  $BW$  at 353.7 cell/ms assuming 150 Mbit/s ATM link. At the switch, its buffer size  $BL$  is assumed to be infinite for the purpose of obtaining the maximum queue length. Both high and low threshold values  $Q_H$  and  $Q_L$  are fixed at 150Kbyte. At each source end system,  $N_{RM}$  is set to 32.

We first examine the effect of the propagation delay on the ramp-up time. In Fig. 3, we plot  $ACR^n(t)$  for  $\tau_1 = \tau_2 = 0.02$  ms. In this figure,  $RIF = 1/64$  and  $RDF = 1/16$  (i.e.,  $RIF_n = 1/64$  and  $RDF_n = 1/16$ ) are chosen to satisfy two objectives — preventing cell loss and achieving full link utilization — for connections of group 1 [5]. We add group 2 to the network when group 1 is at the beginning of Phase 1. In Fig. 4, we change only the round-trip delay of group 2,  $\tau_2$ , from 0.02 ms to 2.00 ms. In Table 1, we also show effective throughput normalized by the link capacity for connections in each group where  $\tau_1$  is fixed at 0.02 ms but  $\tau_2$  is varied as 0.02 ms, 0.20 ms and 2.00 ms. From these results, one can find that the difference in round-trip delays of group 2 has little effect on fairness and the ramp-up time. For example, the ramp-up time in Fig. 4 is almost equivalent to Fig. 3.

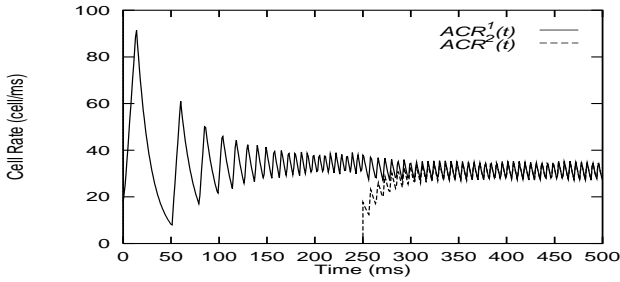


Fig. 3: Effect of Propagation Delay for  $\tau_1 = 0.02$  ms and  $\tau_2 = 0.02$  ms.

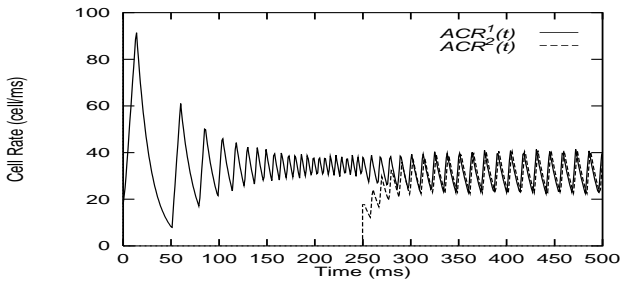


Fig. 4: Effect of Propagation Delay for  $\tau_1 = 0.02$  ms and  $\tau_2 = 2.00$  ms.

The effect of  $RIF$  and  $RDF$  on the additional ABR connection is next investigated. Figure 5 shows the case where a larger value of  $RDF$  is used; that is, the rate decrease is faster than the case of Fig. 3. Here,  $RDF = 1/4$  is used instead of  $1/16$  while

Table 1: Effective Throughput for Each Group.

Round-Trip Delay of Group 2 ( $\tau_2$ )	Group 1	Group 2
0.02 ms	0.0880	0.0880
0.20 ms	0.0880	0.0880
2.00 ms	0.0882	0.0875

$RIF = 1/64$  is unchanged. On the other hand, slower rate increase is considered in Fig. 6 where we use  $RIF = 1/256$  and  $RDF = 1/16$ . These parameter sets are also chosen to prevent cell loss and achieve full link utilization. It can be found that the ramp-up time of group 2 is considerably affected by the setting of  $RIF$  and  $RDF$ . Namely, the ramp-up time becomes shorter by increasing  $RDF$ , and longer by decreasing  $RIF$ . Especially, the small value of  $RIF$  leads to much larger ramp-up time as can be observed in Fig. 6. Therefore, for fulfilling good responsiveness,  $RIF$  and  $RDF$  should be set to large values as long as no cell loss and full link utilization can be satisfied.

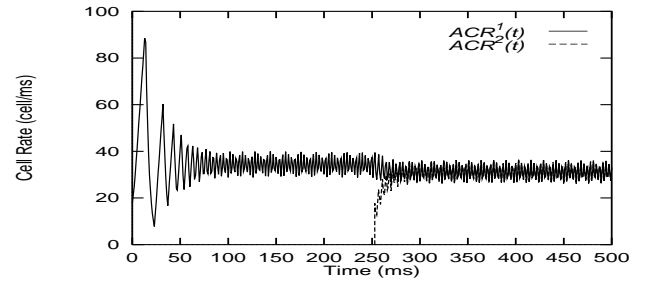


Fig. 5: Effect of Control Parameters for  $RIF = 1/64$  and  $RDF = 1/4$ .

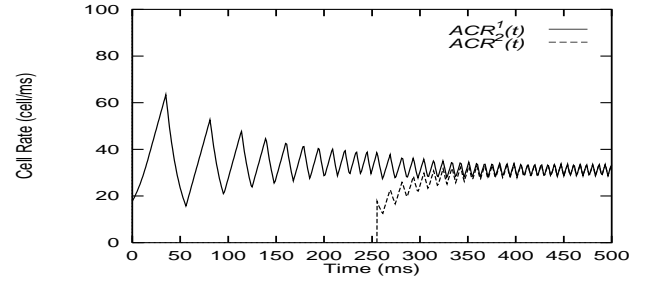


Fig. 6: Effect of Control Parameters for  $RIF = 1/256$  and  $RDF = 1/16$ .

### III. EFFECT OF CBR TRAFFIC

In this section, by extending analytic results obtained in [5], we derive the maximum queue length at the switch when a CBR connection is newly established.

#### A. Analysis

We add a CBR connection to the model presented in Subsection II with  $N = 1$  (see Fig. 1) at time  $t'$  with a fixed bandwidth  $p \times BW$  ( $0 \leq p \leq 1$ ). The available bandwidth to ABR traffic is therefore suddenly changed from  $BW$  to  $(1 - p)BW$  at the

time  $t'$ . Let us introduce  $Q_{max}$  as the maximum queue length after the establishment of the CBR connection at the time  $t'$ . First,  $Q_{max}$  is given by

$$Q_{max} = Q(t' + \tau_{sx}) + \int_{t' + \tau_{sx}}^{t'_{max}} (N_{VC} ACR'(x - \tau_{sx}) - (1-p)BW) dx, \quad (1)$$

where  $ACR'(t)$  is defined as the allowed cell rate  $ACR$  at time  $t (\geq t')$ , and  $t'_{max}$  is the time when  $Q(t)$  takes its maximum value (see Fig. 7). Since  $Q(t)$  starts to decrease again after  $\tau_{sx}$  from when the aggregate cell rate of ABR connections is decreased to  $(1-p)BW$ ,  $t'_{max}$  is obtained as

$$t'_{max} = ACR'^{-1} \left[ \frac{(1-p)BW}{N_{VC}} \right] + \tau_{sx},$$

where  $ACR'^{-1}(x)$  is the inverse representation of  $ACR'(t)$ .

After the time  $t'$ , each source receives backward RM cells with a fixed interval since the switch has always cells in the buffer. By letting  $T_{RDF}$  be the interval of two successively received backward RM cells at the source end system,  $T_{RDF}$  is given by  $N_{RM} N_{VC} / ((1-p)BW)$ . However, when the arrival rate of the backward RM cell is too slow, each source end system decreases its rate by  $CDF$  (Cutoff Decrease Factor) [1]. In particular, when it receives no backward RM cell after transmitting the number  $C_{RM}$  of forward RM cells, it begins to reduce its  $ACR$  at each forward RM cell transmission as

$$ACR \leftarrow \max(ACR - ACR \times CDF, MCR). \quad (2)$$

The main purpose of the rate reduction mechanism introduced by  $C_{RM}$  and  $CDF$  is to allow the source end system to emit cells before receiving the first backward RM cell in its initial transient state [1]. Thus,  $C_{RM}$  may be set to a rather large value. However, as will be shown in numerical examples, this mechanism is also helpful to avoid cell loss for ABR connections caused by background traffic such as CBR traffic.

By letting  $T_{CDF}$  denote the duration of transmitting  $C_{RM}$  forward RM cells without receipt of backward RM cells,  $T_{CDF}$  is given by  $N_{RM} C_{RM} / ACR$ . According to the relation between  $T_{RDF}$  and  $T_{CDF}$ ,  $ACR'(t)$  is obtained as follows.

- $T_{RDF} \leq T_{CDF}$

In this case, since the source end system receives one or more backward RM cells before transmitting  $C_{RM}$  forward RM cells,  $ACR'(t)$  is equivalent to  $ACR_1(t)$  in Phase 1. Therefore, we have

$$ACR'(t) = ACR(t') e^{-\frac{(1-p)BW RDF}{N_{VC} N_{RM}} (t-t')}.$$

- $T_{RDF} > T_{CDF}$

In this case, no backward RM cell is received by the source end system before transmitting  $C_{RM}$  forward RM cells. After the time  $(t' + T_{CDF})$ , the source end system decreases its rate according to Eq.(2) for each forward RM cell transmission. Thus, we have a differential equation as

$$\frac{dACR'(t)}{dt} = -\frac{(ACR'(t))^2 CDF}{N_{RM} C_{RM}}.$$

By solving these equations, we have

$$ACR'(t) = \begin{cases} ACR(t'), & t' \leq t < t' + T_{CDF} \\ \left( \frac{CDF}{N_{RM}} (t-t') + \frac{1}{ACR(t')} \right)^{-1}, & t' + T_{CDF} \leq t \end{cases}$$

Actually, the backward RM cell arrives at the source end system at  $t = t' + T_{RDF}$ , and it decreases  $ACR$  by  $RDF$ . In the above analysis, we ignored the rate reduction by receiving backward RM cells at the source end system since the arrival rate of backward RM cells is slow enough, and  $RDF$  is usually smaller than  $CDF$ . Furthermore, even in the case where  $RDF$  is not small compared with  $CDF$ , our analysis gives the upper-bound of the maximum queue length.

As can be found from Eq. (1),  $Q_{max}$  depends on the initial values such as  $Q(t' + \tau_{sx})$  and  $ACR'(t')$  that further depends on time  $t'$ . In what follows, we derive the maximum of  $Q_{max}$  for any  $t'$ , which is defined as

$$Q'_{max} = \max_{t'}(Q_{max}). \quad (3)$$

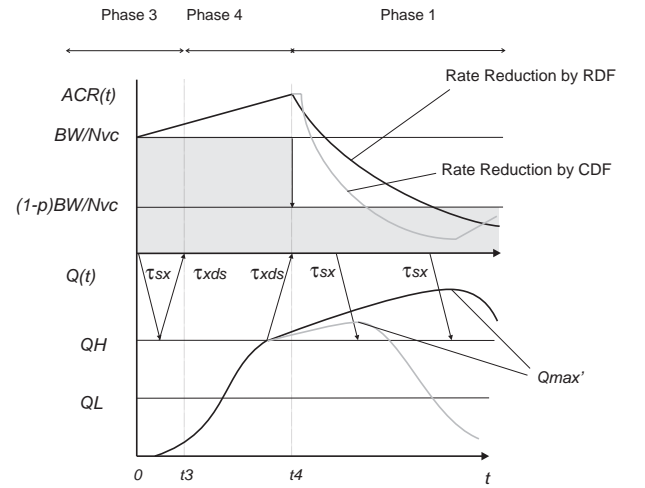


Fig. 7: Pictorial View of  $ACR(t)$  and  $Q(t)$  with CBR Traffic.

As shown in Fig. 2,  $ACR$  takes its maximum value at the end of Phase 4 (at the beginning of Phase 1). In addition,  $ACR'(t)$  is maximized when the switch is not fully utilized since the large amplitude of  $Q(t)$  means the large amplitude of  $ACR(t)$ . Therefore,  $Q'_{max}$  is obtained by setting  $t' = t_4$ , and by giving initial values of Phase 4 as

$$ACR(t_3) = \frac{BW}{N_{VC}},$$

$$Q(t_3 + \tau_{sx}) = 0.$$

At last, we note that the maximum queue length  $Q'_{max}$  is given by a closed-form equation.

### B. Numerical Examples

In the following numerical examples, both  $\tau_{sx}$  and  $\tau_{xd}$  are fixed at 0.005 ms (about 1 km) as a typical value of the LAN environment. Furthermore, the number of ABR connections  $N_{VC}$  is set

to 10. For other control parameters except  $RIF$  and  $RDF$ , we use the same values employed in Section II.

We first show the maximum queue length  $Q'_{max}$  obtained by Eq.(3) as a function of  $p$  in Fig. 8. In this figure,  $RIF$  is fixed at  $1/64$ , and  $C_{RM}$  and  $CDF$  is at 32 and  $1/2$ , respectively, while  $RDF$  is varied as  $1/4$ ,  $1/16$  and  $1/64$ . It can be found that  $Q'_{max}$  increases as  $p$  increases at first. For example, once a CBR connection that requires a half of the link bandwidth (75Mbit/s, in this case) is added, the switch should have 17,000 cells of buffer capacity to avoid cell loss of ABR connections with  $RDF = 1/16$ . Then,  $Q'_{max}$  is suddenly reduced around  $p = 0.9$ . It is because the source end system decreases its rate by  $CDF$  rather than  $RDF$  when the available bandwidth for ABR connections becomes too small. Moreover, one can find that the maximum queue length can be reduced by setting  $RDF$  to a large value (i.e., faster rate decrease). In Fig. 9,  $RIF$  is changed from  $1/64$

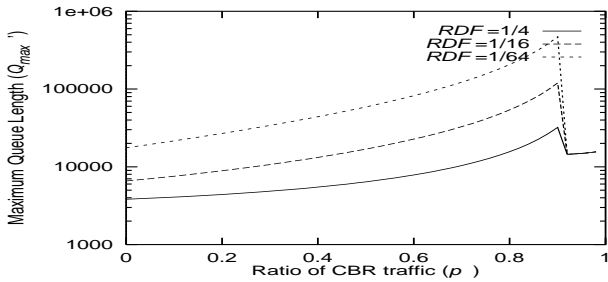


Fig. 8: The Maximum Queue Length vs. Ratio of CBR Traffic for  $RIF = 1/64$  and  $C_{RM} = 32$ .

to  $1/1024$ , which means slower rate increase. In this figure, the maximum queue length is decreased to some extent when compared with Fig. 8. However, a large amount of buffer capacity is still required to prevent cell loss if  $p$  is large.

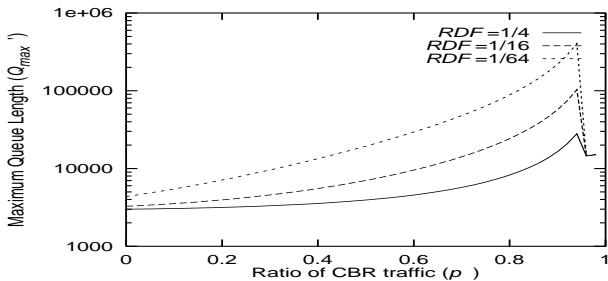


Fig. 9: The Maximum Queue Length vs. Ratio of CBR Traffic for  $RIF = 1/1024$  and  $C_{RM} = 32$ .

By setting  $C_{RM}$  properly, cell loss can be prevented even when the CBR connection reserves the bandwidth close to the link capacity as shown in Fig. 10. In this figures,  $RIF$  is set to  $1/64$  but  $C_{RM}$  that decides the duration to rate reduction by  $CDF$  is changed from 32 to 4. This figure shows that the maximum queue length can be limited even when  $p$  becomes large. For example, 12,000 cells of the buffer capacity is sufficient for preventing cell loss with  $RDF = 1/16$  even when the CBR connection requires the entire bandwidth.

From the above observations, we can conclude that to limit

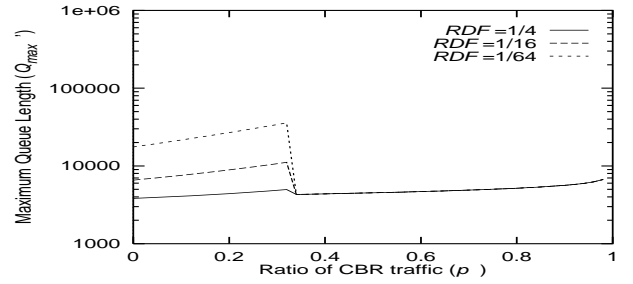


Fig. 10: The Maximum Queue Length vs. Ratio of CBR Traffic for  $RIF = 1/64$  and  $C_{RM} = 4$ .

the queue buildup by a new CBR connection, each of  $RIF$  and  $RDF$  should be small and large, respectively. Moreover, a smaller value of  $C_{RM}$  is helpful to prevent cell loss.

## IV. CONCLUSION

In this paper, we have presented two sorts of analyses. One was the analysis for the model with several groups of connections with different propagation delays in order to reveal the fairness problem among connections and the ramp-up time of an additional ABR connection. The other was the derivation of the maximum queue length at the switch buffer affected by an addition of background traffic such as CBR traffic. Through numerical examples, we have shown that a large value of  $RIF$  (i.e., fast rate increase) is helpful to shorten the ramp-up time, and that a small value of  $C_{RM}$  dramatically reduces the maximum queue length caused by background traffic.

## REFERENCES

- [1] The ATM Forum Technical Committee, "Traffic management specification version 4.0 (draft version)," *ATM Forum Contribution 95-0013R10*, February 1996.
- [2] H. Ohsaki, M. Murata, H. Suzuki, C. Ikeda, and H. Miyahara, "Rate-based congestion control for ATM networks," *ACM SIGCOMM Computer Communication Review*, vol. 25, pp. 60–72, April 1995.
- [3] R. Jain, "Congestion control and traffic management in ATM networks: recent advances and a survey," *ATM Forum Contribution 95-0177*, 1995.
- [4] H. Ohsaki, M. Murata, H. Suzuki, C. Ikeda, and H. Miyahara, "Analysis of rate-based congestion control methods in ATM networks, Part 1: steady state analysis," *IEEE GLOBECOM '95*, pp. 296–303, November 1995.
- [5] H. Ohsaki, M. Murata, H. Miyahara, C. Ikeda, and H. Suzuki, "Parameter tuning for binary mode switch — analysis," *ATM Forum Contribution 95-1483*, 1995.
- [6] C. Ikeda, H. Suzuki, H. Ohsaki, and M. Murata, "Recommendation parameter set for binary switch," *ATM Forum Contribution 95-1482*, December 1995.
- [7] J.-C. Bolot and A. U. Shankar, "Dynamical behavior of rate-based flow control mechanisms," *Computer Communication Review*, vol. 20, pp. 35–49, 4 1990.